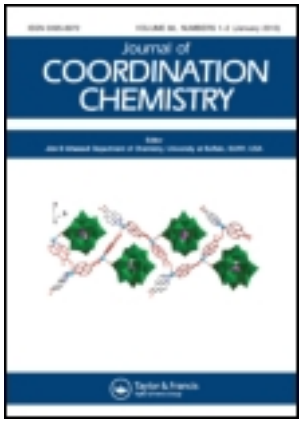

Journal of Coordination Chemistry
Publication details, including instructions for authors and subscription information:
http://www.tandfonline.com/loi/gcoo20

DNA binding ad photocleavage properties of cationic porphyrin-polypyridyl ruthenium(II) hybrids

Ping Zhao[a], Jun Li[b], Li-Jun Yang[c], Jia-Zheng Lu[d], Hai-Min Guo[a], Li-Na Ma[a] & Bing-Hui Ou[a]

[a] School of Chemistry and Chemical Engineering, Guangdong Pharmaceutical University, Zhongshan, PR China

[b] Department of Chemistry, Guangdong University of Education, Guangzhou, PR China

[c] Department of Gynecology and Obstetrics, Zhongshan People' Hospital, Zhongshan, PR China

[d] School of Pharmacy, Guangdong Pharmaceutical University, Guangzhou, PR China

Published online: 04 Dec 2013.

To cite this article: Ping Zhao, Jun Li, Li-Jun Yang, Jia-Zheng Lu, Hai-Min Guo, Li-Na Ma & Bing-Hui Ou (2013) DNA binding ad photocleavage properties of cationic porphyrin-polypyridyl ruthenium(II) hybrids, Journal of Coordination Chemistry, 66:23, 4220-4236, DOI: 10.1080/00958972.2013.866234

To link to this article: http://dx.doi.org/10.1080/00958972.2013.866234

Journal of Coordination Chemistry, 2013
Vol. 66, No. 23, 4220–4236, http://dx.doi.org/10.1080/00958972.2013.866234

DNA binding ad photocleavage properties of cationic porphyrin-polypyridyl ruthenium(II) hybrids

PING ZHAO*†, JUN LI‡, LI-JUN YANG§, JIA-ZHENG LU¶, HAI-MIN GUO†, LI-NA MA† and BING-HUI OU†

†School of Chemistry and Chemical Engineering, Guangdong Pharmaceutical University, Zhongshan, PR China
‡Department of Chemistry, Guangdong University of Education, Guangzhou, PR China
§Department of Gynecology and Obstetrics, Zhongshan People' Hospital, Zhongshan, PR China
¶School of Pharmacy, Guangdong Pharmaceutical University, Guangzhou, PR China

(*Received 22 August 2013; accepted 31 October 2013*)

Three cationic porphyrin-polypyridyl ruthenium(II) hybrids, differing in the planar areas of the polypyridyl moieties, were synthesized and their interactions with DNA investigated using absorption and fluorescence titration, induced circular dichroism spectra, thermal DNA denaturation measurements, as well as surface-enhanced Raman spectroscopy. Ethidium bromide competition experiments determined the binding affinity constants (K_b) of these compounds for CT DNA. DNA photocleavage experiments indicated that these hybrids have a broader cleaving wavelength range than traditional drugs and $^1O_2$ is the reactive species responsible for the cleavage. The proper planar area was proved to be responsible for the larger K_b and higher DNA photocleavage efficiency.

Keywords: Porphyrin-polypyridyl ruthenium(II) hybrids; DNA binding; DNA photocleavage

1. Introduction

Because of their unique ability of accumulation in tumor tissues and marked photochemical nuclease activity, porphyrins play an important role in anti-cancer agents [1, 2]. Cationic porphyrins, represented by *meso*-tetrakis(4-*N*-methylpyridiniumyl)porphyrin (TMPyP), have attracted considerable attention for their additional tight interaction and efficient photocleavage with DNA. The special DNA binding and cleaving properties make TMPyP an ideal model for the DNA-binding agents utilized in photodynamic therapy of tumors [3–5]. Recently, TMPyP has been reported to be coupled with other bioactive molecules and thus greatly improved the biochemical properties of these small drugs [6–8]. We have also systemically investigated the duplex and G-quadruplex DNA binding behaviors of a TMPyP-like structure bearing an anthraquinone chromophore (Por-AQ) [9–11].

Ruthenium(II) polypyridine complexes, due to a combination of easily constructed rigid chiral structures spanning all three spatial dimensions and a rich photophysical repertoire, are regarded as promising candidates and several ruthenium complexes have now been proposed as potential anticancer substances [12–14]. It is well established

*Corresponding author. Email: zhaoping666@163.com

that the DNA binding affinity of the ruthenium(II) polypyridine complex is a very important factor in the study of the anticancer properties and higher DNA binding efficiency often related to better antitumor abilities [15, 16]. Thus, efforts on promoting the DNA interaction abilities of ruthenium(II) polypyridine complexes mushroomed in the past decades and most of them concentrated on modifying the ligands or changing substituents of polypyridine [17–20]. Liu and Liu *et al.* have investigated Ru(II) complexes with dppz-based or bipyridine ligands and found that different substituents on ligands will affect the DNA binding affinities of the compounds [21, 22]. Paul and Shilpa *et al.* have reported Ru(II) complexes with pyrrol-azo or dipyridophenazine ligands and researched their interactions with DNA and BSA [23, 24]. All of these reports focused on the biochemical characters of single-cored Ru(II) complexes, with the only difference on the coordinating ligands or the substituents on the ligands. However, up to now, reports on the DNA interaction behaviors of molecules constructed with both Ru(II) complexes and other bioactive drugs are relatively rare. In the last decade, there is some research on porphyrin-polypyridyl Ru(II) (PPRu) compounds assembled through the coordination of the ruthenium(II) center with the substituents of porphyrin. It is reported that these compounds have distinctive DNA-binding properties from the simple polypyridyl Ru(II) complex [25–27]. So far there are no reports focused on DNA-binding properties of the hybrid covalently linked with the porphyrin ring and polypyridyl Ru(II) complex.

Our promising results on Por-AQ hybrids encouraged us to link the TMPyP-like structure to polypyridyl Ru(II) complexes with flexible chains and it is supposed that the covalently linked porphyrin-polypyridyl Ru(II) (PPRu) hybrids will bring us new information on their biochemical properties. Herein, three PPRu hybrids with different polypyridyl ligands have been synthesized and their binding as well as photocleavage properties to DNA were investigated. Absorption and fluorescence titration, surface-enhanced Raman spectroscopy (SERS) and induced circular dichroism (ICD) spectral measurements were synthetically used here.

2. Experimental and methods

2.1. *Materials and chemicals*

CT DNA and pBR322 supercoiled plasmid DNA were obtained from the Sigma Company. Buffer A (5 mM Tris-HCl, 50 mM NaCl, pH = 7.2, Tris = Tris(hydroxymethyl)aminomethane) solution was used in spectral, equilibrium dialysis and EB competition experiments and buffer B (1.5 mM Na_2HPO_4, 0.5 mM NaH_2PO_4, 0.25 mM Na_2H_2EDTA, pH = 7.0, H_4EDTA = N,N′-ethane-1,2-diylbis[N-(carboxymethyl)glycine]) was employed for thermal denaturation studies. Gel electrophoresis studies were carried out in buffer C (50 mM Tris-HCl, 18 mM NaCl, pH = 7.2). A solution of CT DNA in buffer A gave a ratio of UV absorbance at 260 and 280 nm of 1.85:1, indicating that the CT DNA was sufficiently free of protein [28]. The CT DNA concentration per nucleotide was determined by absorption spectroscopy using the molar absorption coefficient (6600 M^{-1} cm^{-1}) at 260 nm [28].

2.2. *Measurements*

Electrospray ionization mass spectra (ESI–MS) were recorded on a LCQ DECA XP system (Thermo, USA). ^{1}H NMR spectra were recorded on a Varian-300 spectrometer. All chemical shifts are given relative to tetramethylsilane (TMS). Elemental analyses (C, H and N) were carried out with a Perkin-Elmer 240 Q elemental analyzer. UV–Vis spectra were recorded on a Perkin-Elmer-Lambda-850 spectrophotometer. Emission spectra were recorded on a Perkin–Elmer L55 spectrofluorophotometer. SERS spectra were carried out on a Laser Micro-Raman Spectrometer of Renishaw in Via, with a power of 20 mW at the samples. CD spectra were recorded on a JASCO-J810 spectrometer.

SERS experiment: Ag colloids were prepared by reducing $AgNO_3$ with EDTA according to the reported method [29]. The Ag colloid/compound (or Ag colloid/DNA) SERS active systems were prepared by mixing equal volumes of the compound (or DNA) solutions with the Ag colloid in buffer A to obtain the desired compound or DNA concentrations. In the compound/DNA complex experiments, the solution of DNA was mixed with the PPRu hybrid solution at a DNA/compound ratio of 30:1, then an equal volume of the mixed solution was fully mixed with the Ag colloid, and the spectrum was immediately measured at room temperature. The final concentrations of compounds and DNA in all of the SERS-active systems were 5 and 150 μM, respectively.

Equilibrium dialysis experiment: A volume of 100 ml dialysate buffer solution (10 mM sodium phosphate, pH 7.0) containing 50 μM hybrid (C_t) was placed in a conical flask. Extinction coefficient of the Soret band of the hybrid was then spectrophotometrically determined. A 5 ml dialysate buffer solution containing CT DNA (0.5 mM) was pipetted into a dialysis bag, which was then soaked in the 100 ml hybrid solution. The conical flask was then airproofed, and its content was allowed to equilibrate with stirring for 24 h at 25 °C. After the completion of equilibration, the free hybrid concentration (C_f) was determined spectrophotometrically. The amount of bound hybrid (C_b) was determined by the difference, $C_b = C_t - C_f$.

For the gel electrophoresis experiment, a high pressure mercury lamp-light filter assembly was used. Yellow light filter was used for visible light ($\lambda > 470$ nm) and purple filter for ultraviolet light ($\lambda < 350$ nm) [30]. The samples were analyzed by electrophoresis for 2.5 h at 80 V in Tris-acetate buffer containing 1% agarose gel. The gel was stained with 1 μg ml^{-1} EB and photographed under UV light.

2.3. *Synthesis*

The synthetic route to **1**, **2** and **3** is shown in scheme 1. 5-(4-Hydroxyphenyl)10,15,20-tris (4-N-pyridiniumyl)porphyrin (HTPyP) was previously synthesized [31]. Ip (imidazo-[4,5-f] [1, 10]phenanthroline), $[Ru(pip)_2](ClO_4)_2 \cdot 3H_2O$, $[Ru(phen)_2](ClO_4)_2 \cdot 3H_2O$ and $[Ru(bpy)_2]Cl_2 \cdot 3H_2O$ were synthesized and purified by published methods [32, 33].

2.3.1. Synthesis of (BrBPTPyP). 130 mg HTPyP (0.21 mM) was dissolved in 6 mL N,N-dimethylformamide (DMF). Then, Na_2CO_3 (100 mg) and dibromobutane (110 mg, 0.50 mM) were added. The reaction mixture was stirred at room temperature for 28–36 h. The progress of the reaction was monitored by TLC. After the reaction was complete, the reaction mixture was diluted with $CHCl_3$ and poured into water. The organic layer was separated and washed with water until neutral pH, dried over anhydrous Na_2SO_4,

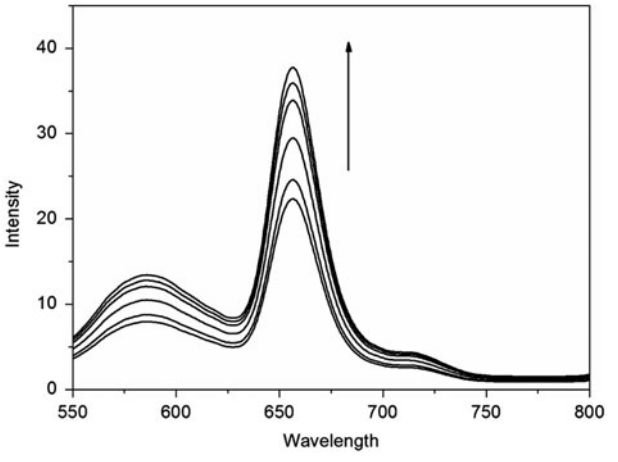

Figure 1. Emission spectra for Por moiety of **1** in the absence and presence of CT DNA in buffer A. [PPRu] = 10 μM. Arrows show the intensity change upon increasing DNA concentrations. λ_{ex} = 449 nm.

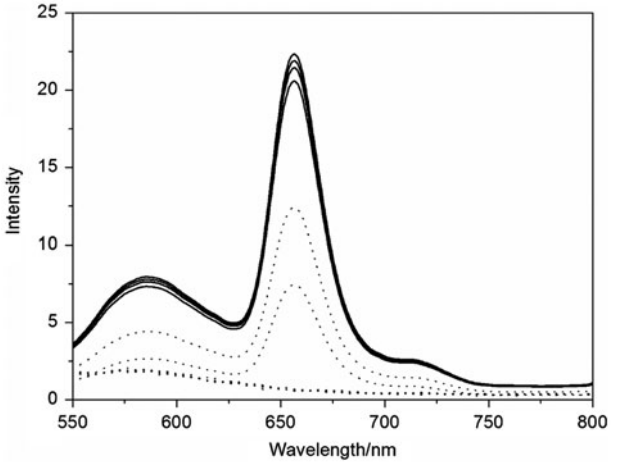

Figure 2. Emission quenching with $K_4Fe(CN)_6$ for free **3** (dotted line) and DNA-bound **3** (solid line) in buffer A. I_0 and I are the fluorescence intensities of the compounds in the absence and presence of $K_4Fe(CN)_6$. [PPRu]/[DNA] = 0.25.

and evaporated under diminished pressure. The crude product was purified by column chromatography. The final product was isolated as the objected BrBPTPyP (5-(1-bromobutylhydroxylphenyl)-10,15,20tris(4-pyridiniumyl)porphyrin) in 76.6% yield. ESI-MS: *m/z* 767.2 ($[M\text{-}H]^-$).

2.3.2. Synthesis of (C_4ip)TPyP. A mixture of BrBPTPyP (100 mg, 0.13 mM), Ip (500 mg, 2.27 mM) and K_2CO_3 (1 g) was stirred for 48 h in 30 ml DMF at room temperature. Then, the reaction mixture was diluted with $CHCl_3$ (40 ml) and washed with H_2O. After drying

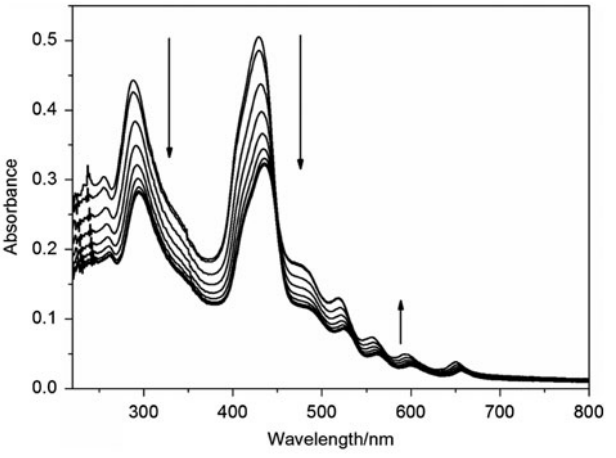

Figure 3. Absorption spectra of **2** in buffer A at 25 °C in the presence of increasing amounts of CT DNA. [PPRu] = 10 μM. Arrows indicate the change in absorbance upon increasing DNA concentration.

over anhydrous Na_2SO_4 and concentrating via rotary evaporation, the residue was chromatographed on a silica gel column using $CHCl_3$ and MeOH as eluent. The main purple band was collected as (C_4ip)TPyP (5-[p-(imidazo[4,5-f][1,10]phenanthroline)butoxyl]-phenyl-10,15,20-tris(4pyridiniumyl)porphyrin). Yield: 71.3%. ESI-MS: *m/z* 908.3 ($[M\text{-}H]^-$).

2.3.3. Synthesis of 1, 2 and 3. Compound **1**: (C_4ip)TPyP (91 mg, 0.10 mM) and *cis*-$[Ru(phen)_2]Cl_2{\cdot}3H_2O$ (0.059 g, 0.10 mM) were mixed and refluxed for ca. 1 h in HAc (10 ml) under an Ar atmosphere. After removing the solvent by rotary evaporation, the solid residue was redissolved in a minimum volume of MeOH which was refluxed for 1 h. The product was then precipitated by adding a saturated solution of $KClO_4$, filtered and further dried under vacuum to get a red solid. The crude product was purified by column chromatography on alumina using $CHCl_3$. EtOH (20:1, V/V) as eluent, the main brown-red band was collected and dried in vacuum. The product was methylated in 5 ml DMF with methyl iodide (0.8 ml) for 3 h at room temperature. The solvent and methyl iodide were removed under vacuum. Compound **1** was thus obtained quantitatively. Yield: 0.105 g, 65.8%. ESI-MS: *m/z* 684.5 ($[M\text{-}2ClO_4]^{2+}$). (Found: C, 50.54; H, 3.42; N, 10.29%. Calcd for $[RuC_{85}H_{70}I_3ON_{15}](ClO_4)_2{\cdot}2H_2O$: C, 50.28; H, 3.48; N, 10.35%). ^{1}H NMR (500 MHz, DMSO): chemical shift δ: 9.39 (d, J = 5.9 Hz, 6H, 2, 6-pyridinium), 9.04 (d, J = 6.6 Hz, 4H, β-pyrrole), 8.90 (s, 6H, 3,5-pyridinium), 8.65 (s, 2H, 2, 6-phenyl), 8.01 (s, 2H, β-pyridinium H), 7.78 (s, 4H, β-pyridinium H), 7.36 (s, 4H, phenyl), 7.15 (s, α-pyridinium H), 6.80 (s, 6H, β-pyridinium H), 4.73 (s, 9H, N^+–Me), 4.35 (s, 2H, CH_2–N), 3.97 (s, H, O–CH_2–), 1.18–1.90 (m, 4H, –$(CH_2)_2$–), –3.10 (s, 2H, NH pyrrole). IR (KBr, cm^{-1}): 3316 (ν_{N-H}), 3059, 3031, 2930, 2866 (ν_{C-H}), 1609, 1466 ($\nu_{C=C}$), 1242 (ν_{C-O}), 1175, 966 (δ_{C-H}), 1090 (ν_{ClO_4}), 848 (ν_{phen}), 758 (ν_{bpy}), 621 (δ_{ClO_4}). (The 1D H and 2D HH, CH Cosy spectra of these compounds are given in Supplementary material (see online supplemental material at http://dx.doi.org/10.1080/00958972.2013.866234), in which the specific ^{1}H assignments are given in detail.)

Compounds **2** and **3** were similarly prepared, replacing *cis*-$[Ru(phen)_2]Cl_2{\cdot}3H_2O$ with $[Ru(pip)_2](ClO_4)_2{\cdot}3H_2O$ and $[Ru(bpy)_2]Cl_2{\cdot}3H_2O$, respectively.

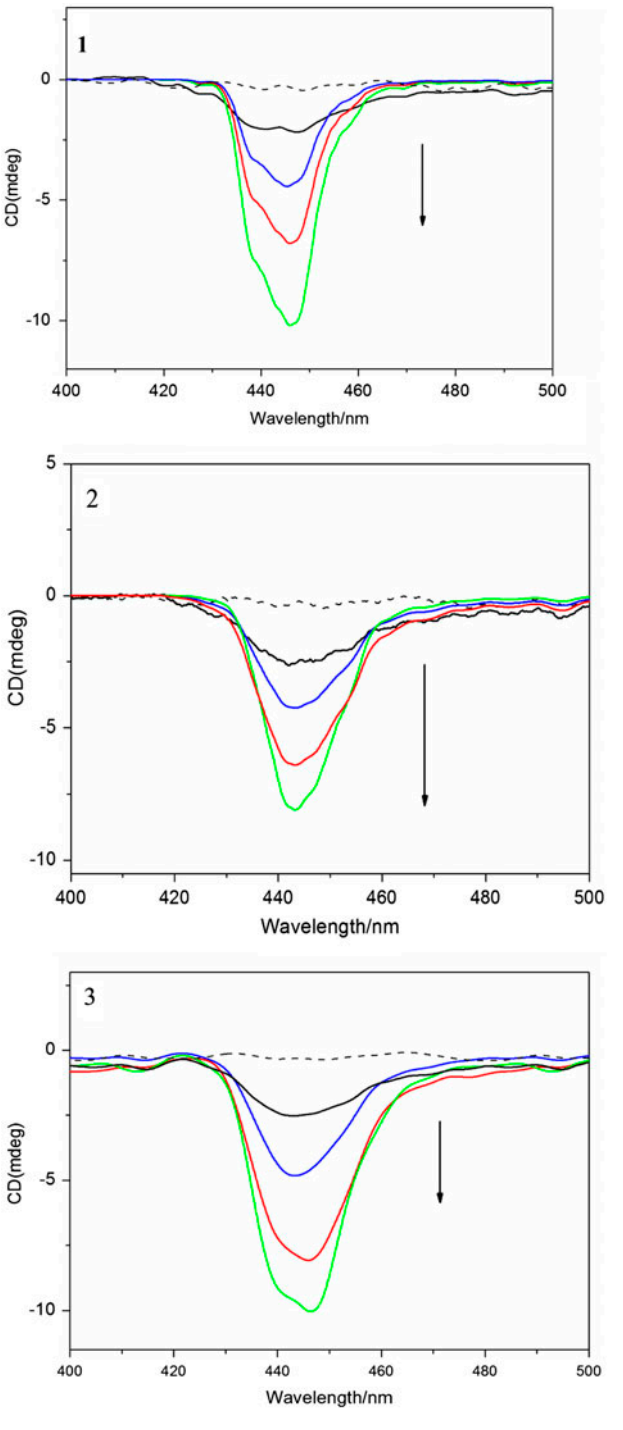

Figure 4. ICD spectra of PPRu hybrids in the absence (dotted line) and presence (solid line) of CT DNA in buffer A. [PPRu] = 10 μM, [PPRu]/[DNA] = 0.2 (—), 0.15 (—), 0.10 (—), 0.05 (—). Arrows indicate the change in ICD spectra upon increasing DNA concentration.

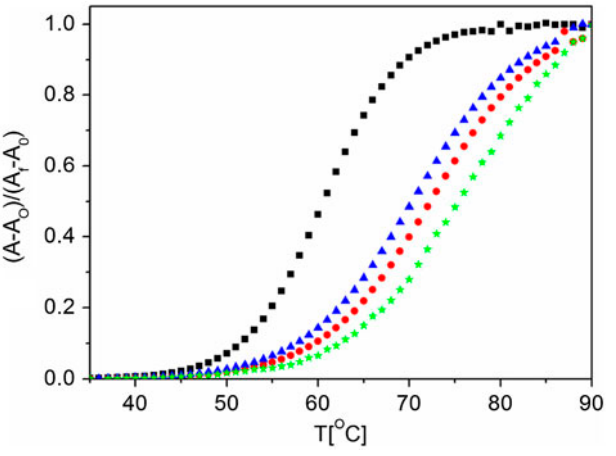

Figure 5. Melting curves of CT DNA at 260 nm in the absence (■) and presence of **1** (★), **2** (▲) and **3** (●) in buffer B. [PPRu] = 10 μM, [DNA] = 100 μM.

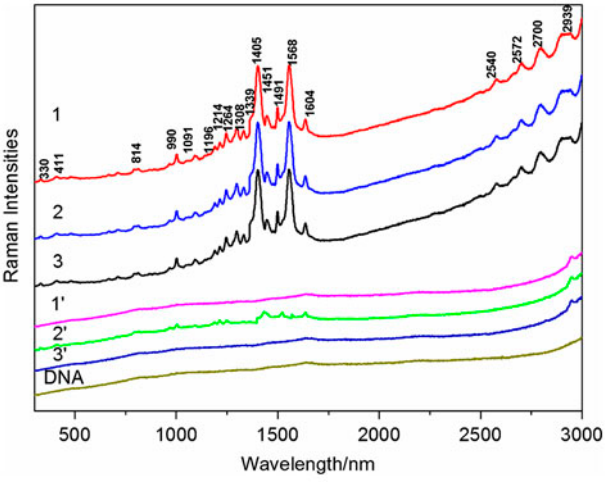

Figure 6. SERS spectra (250-3000 cm^{-1}) of CT DNA and PPRu hybrids in the absence (1–3) and presence (1′–3′) of CT DNA. (1), (2) and (3) for free **1**, **2** and **3**, respectively; (1′), (2′) and (3′) for DNA complexes with **1**, **2** and **3**, respectively. [DNA]/[PPRu] = 30:1.

2: ESI-MS: *m/z* 800.1 ([M-2ClO$_4$]$^{2+}$). (Found: C, 51.89; H, 3.57; N, 11.63%. Calcd for [RuC$_{99}$H$_{82}$I$_3$ON$_{19}$](ClO$_4$)$_2$·4H$_2$O: C, 51.73; H, 3.60; N, 11.58%.) ^{1}H NMR (500 MHz, DMSO): chemical shift δ: 9.37 (d, J = 5.9 Hz, 6H, 2, 6-pyridinium), 9.20 (s, 4H, β-pyrrole), 9.01 (d, J = 6.6 Hz, 4H, β-pyrrole), 8.88 (s, 6H, 3,5-pyridinium), 8.64 (s, 2H, 2, 6-phenyl), 7.95 (s, 2H, 3,5-phenyl), 7.78 (s, 4H, β-pyridinium H), 7.46–7.36 (s, 10H, phenyl), 7.15 (s, α-pyridinium H), 6.79 (s, 6H, β-pyridinium H), 4.72 (s, 9H, N$^+$–Me), 4.33 (s, 2H, CH$_2$–N), 3.95 (s, H, O–CH$_2$–), 3.53 (s, 2H, NH), 1.18–1.90 (m, 4H, –(CH$_2$)$_2$–), –2.98 (s, 2H, NH pyrrole). IR (KBr, cm^{-1}): 3312 (ν_{N-H}), 3055, 3031, 2930, 2866 (ν_{C-H}), 1609, 1469 ($\nu_{C=C}$), 1242 (ν_{C-O}), 1175, 968 (δ_{C-H}), 1090 (ν_{ClO_4}), 848 (ν_{phen}), 621 (δ_{ClO_4}).

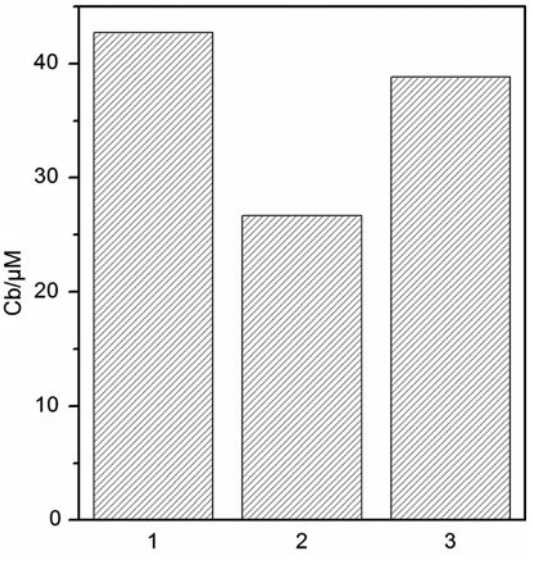

Figure 7. The amounts of PPRu hybrids bound to CT DNA (C_b) in dialysate buffer (10 mM sodium phosphate, pH 7.0). Columns 1, 2 and 3 for hybrids **1**, **2** and **3**, respectively. [DNA] = 0.5 mM, C_t = 50 μM, dialyse for 24 h at 25 °C.

3: ESI-MS: *m/z* 700.8 ($[M\text{-}2ClO_4]^{2+}$). (Found: C, 48.44; H, 3.63; N, 10.47%. Calcd for $[RuC_{81}H_{74}I_3ON_{15}](ClO_4)_2{\cdot}4H_2O$: C, 48.20; H, 3.70; N, 10.41%). ^{1}H NMR (500 MHz, DMSO): chemical shift δ: 9.35 (d, J = 5.9 Hz, 6H, 2, 6-pyridinium), 9.19 (s, 4H, β-pyrrole), 9.02 (d, J = 6.6 Hz, 4H, β-pyrrole), 8.87 (s, 6H, 3,5-pyridinium), 8.61 (s, 2H, 2, 6-phenyl), 8.01 (s, 2H, 3,5-phenyl), 7.36 (s, 4H, phenyl), 4.73 (s, 9H, N^+–Me), 4.34 (s, 2H, CH_2–N), 3.91 (s, H, O–CH_2–), 3.52 (s, 2H, NH), 1.18-1.90 (m, 8H, –$(CH_2)_4$–), –2.96 (s, 2H, NH pyrrole). IR (KBr, cm^{-1}): 3310 (ν_{N-H}), 3059, 3031, 2930, 2878 (ν_{C-H}), 1609, 1466 ($\nu_{C=C}$), 1241 (ν_{C-O}), 1177, 965 (δ_{C-H}), 1090 (ν_{ClO_4}), 844 (ν_{phen}), 758 (ν_{bpy}), 620 (δ_{ClO_4}).

(Caution! Perchlorate salts of metal complexes with organic ligands are potentially explosive, and only small amounts of the material should be prepared and handled with great care.)

3. Results and discussion

3.1. *Synthesis and characterization*

PPRu compounds were easily obtained on the basis of the successful synthetic experience of porphyrin and simple Ru(II) complexes. The porphyrin parent was first attached to brominated flexible carbon chains and then the Ip moiety was linked up effortlessly. Simple Ru(II) complexes, $[Ru(pip)_2](ClO_4)_2{\cdot}3H_2O$, $[Ru(phen)_2](ClO_4)_2{\cdot}3H_2O$ and $[Ru(bpy)_2]Cl_2{\cdot}3H_2O$, were attached to the porphyrin-Ip intermediate product through the coordination of Ru(II) to Ip. The desired products were obtained by final methylation of the porphryin part. The compounds were characterized with EMS, NMR and elemental analysis. This method has the advantages of high productivity and effortlessness, with high purities of the final compounds.

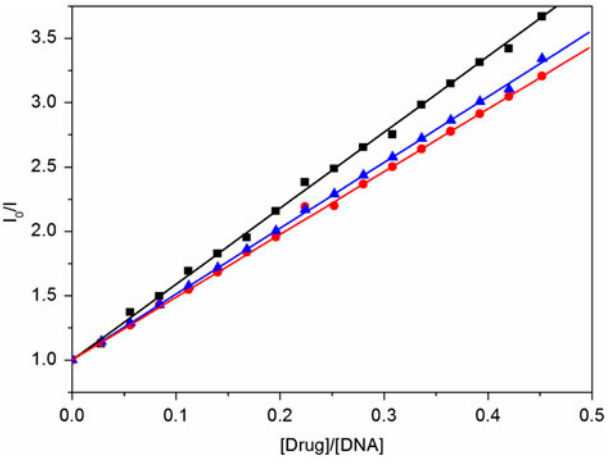

Figure 8. Fluorescence quenching plots of DNA-bound EB by **1** (■), **2** (●) and **3** (▲) in buffer A. [DNA] = 100 μM, [EB] = 16.0 μM, λ_{ex} = 537 nm.

3.2. *DNA-binding properties*

3.2.1. Fluorescence studies. Similar luminescence was emitted by these hybrids at ca. 580 and 660 nm (which were attributed to polypyridyl Ru(II) and porphyrin moieties, respectively) in Tris buffer at room temperature when excited at 449 nm. Fluorescence emission spectrum of **1** is selected to show the spectral change with increasing DNA in figure 1, from which we find that the fluorescence intensities are remarkably enhanced with increase of DNA. Since the hydrophobic environment provided by DNA can protect the compound from quenching by water molecules [34–36], the emission increase is widely admitted as an indication of the interaction between drugs and DNA [35, 36].

3.2.2. Fluorescence emission quenching studies. For drugs with positive charges, steady-state emission quenching experiment was often employed to evaluate the DNA binding of positively charged compounds. Figure 2 gives **3** as an example to illustrate the quenching effect of $K_4Fe(CN)_6$ on the fluorescence intensities of compound in the absence and presence of CT DNA. From figure 2, we find that in the absence of CT DNA, the fluorescence of **3** is significantly quenched at the initial stage of $K_4Fe(CN)_6$ addition and completely dashed with further increase of $[K_4Fe(CN)_6]$. However, in the DNA–drug system, there is no substantial change on the fluorescence intensity of **3** with increasing $K_4Fe(CN)_6$ concentrations. This may be explained by the fact that the bound cations of the compounds are protected from the anionic water-bound quencher by the array of negative charges along the DNA phosphate backbone [37]. Similar results were obtained in the case of **1** and **2**, suggesting that all these compounds can bind to the DNA rather strongly.

3.2.3. Absorption titrations. The association of the cationic PPRu hybrids with CT DNA was examined by absorption titration in the UV-Vis range. The electronic absorption spectra of **1**, **2** and **3** are characterized by Soret and Q bands of the porphyrin moiety, as well as a

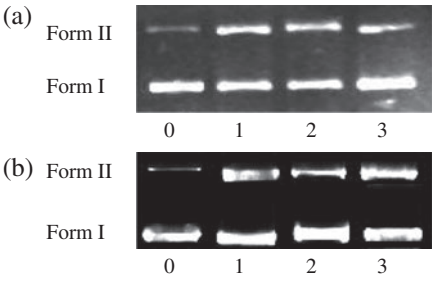

Figure 9. Photocleavage of pBR322 plasmid DNA after irradiation by visible light ($\lambda > 470$ nm) in air (a) or ultraviolet light ($\lambda < 350$ nm) under an Ar atmosphere (b). 10 μL reaction mixtures containing 1.0 μg of plasmid DNA in buffer C. [PPRu] = 2 μM. Lane 0: untreated DNA, no irradiation; lanes 1, 2 and 3: in the presence of **1**, **2** and **3**, respectively, irradiation for 20 minutes.

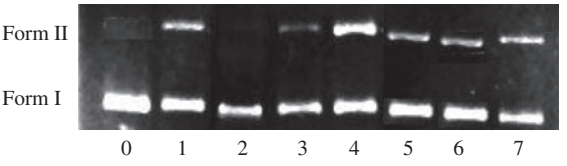

Figure 10. Photocleavage of pBR322 plasmid DNA in the presence of **1** and different inhibitors after irradiation by high pressure mercury lamp-light for 10 min. 10 μL reaction mixtures containing 1.0 μg of plasmid DNA in buffer C. [PPRu] = 2 μM. Lane 0: DNA control; lane 1: in the presence of porphyrin, no inhibitor; lanes 2–6: in the presence of porphyrin and inhibitor: (2) NaN_3 (5 mM), (3) under an Ar atmosphere, (4) 70% D_2O, (5) ethanol (5 mM), (6) methanol (5 mM), (7) DMSO (5 mM).

metal-to-ligand charge transfer (MLCT) and an internal $\pi \rightarrow \pi^*$ ligand transition (IL) of the polypyridyl Ru(II) complex moiety. Figure 3 exemplifies the absorption spectral changes of **2** upon DNA addition. As the concentration of CT-DNA increased, the Soret band and IL band of the three PPRu exhibit significant hypochromism and red shifts. Table 1 summarizes the detailed titration data of all these PPRu compounds **1**, **2** and **3**.

From figure 3 and table 1, one can easily find that with increasing DNA concentration, the absorption spectra of the cationic PPRu hybrids in the Soret band are remarkably disturbed, with great hypochromism and bathochromism. As is well known, the magnitude of spectral perturbation is an intuitional evidence for DNA binding of porphyrins [34]. Intercalation of porphyrin into DNA base pairs is characterized by a large red shift and intensity decrease in the Soret band of UV–Vis spectra; groove binding mode shows no (or minor) change in UV–Vis spectra while outside binding mode also exhibits red shift and intensity decrease in the Soret band of porphyrins [9–11, 34–36]. Thus, the large degree of hypochromism and bathochromism in the Soret bands of PPRu compounds **1**, **2** and **3** indicates that the porphyrin moiety of these PPRu hybrids binds to DNA in an intercalative binding mode.

Similar phenomena were also observed in the polypyridyl Ru(II) complex moieties (ranging from 260 to 350 nm) of the UV–Vis spectra of these compounds. Upon addition of DNA, the changes of absorption spectra in this range are accompanied by large bathochromism with substantial hypochromism.

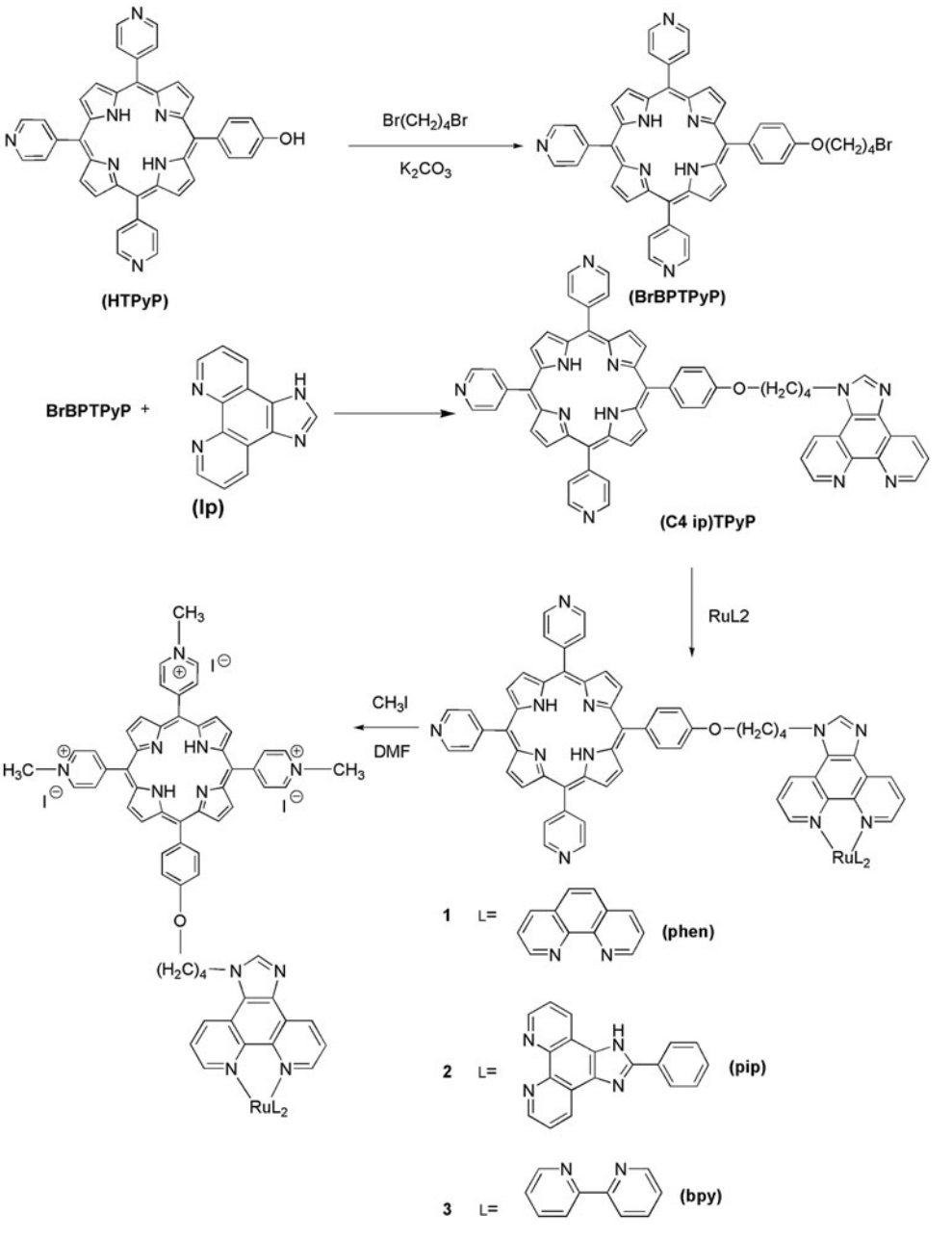

Scheme 1. The synthetic scheme of cationic PPRu hybrids.

From the large spectral perturbation of both porphyrin and polypyridyl Ru(II) moieties, we propose that the two moieties in these PPRu hybrids may both bind to DNA in a classic intercalative mode, whereas a conclusion as to the specific binding mode of these PPRu dyads cannot be made from this method alone.

3.2.4. ICD spectra. It has been reported that the ICD spectra in the Soret range of porphyrins are well-defined indicators for the binding modes toward DNA [3–8, 30]. A positive ICD peak is due to groove binding and a negative ICD peak is due to intercalative binding, whereas a conservative ICD peak is ascribed to the outside binding of porphyrins to DNA [9–11, 34, 35].

Figure 4 illustrates the ICD spectra for PPRu compounds bound to CT DNA in [PPRu]/[DNA] ratio ranging from 0.2 to 0.05. None of these compounds as well as DNA by themselves displays any CD spectral signal in the visible range, but ICD spectra are observed in the Soret band of these compounds with DNA titration. The ellipticities observed for all these compounds in the presence of DNA are predominantly negative in character and centered at the wavelength ranging from 430 to 470 nm. With addition of DNA, the negative signal of ICD spectra becomes stronger. Since the negative ICD signal is diagnostic of intercalative binding, this result confirms that the Por moieties of **1**, **2** and **3** intercalate into the DNA duplex under the experimental conditions. The strong ICD signals of these compounds are in good agreement with the foregoing absorption spectral results.

3.2.5. Thermal denaturation studies. The melting temperature (T_m) of DNA can be used as an indicator of the binding properties and binding strengths of compounds with DNA since T_m is sensitive to DNA double-helix stability and the binding strength of compounds to DNA [12–14, 34]. The thermal denaturation of double-helical polynucleotides from double stranded to single stranded is manifested as hyperchromism in the UV absorption. Upon binding of small molecules to DNA, the T_m value of the B-form DNA should become higher as compared to that of unbound or free DNA. In addition, as the small molecules bind more strongly to the DNA, increase in the T_m value will become larger. Meanwhile, it has been proved that T_m will considerably increase when intercalation binding mode occurs [34].

Table 1. Physical data of PPRu hybrids binding with CT DNA.

Compound	UV–Vis spectra				ΔT_m °C	K_b $\times 10^6$ M^{-1}
	Por		Polypyridyl Ru(II)			
	$\Delta\lambda$ (nm)	H%	$\Delta\lambda$ (nm)	H%		
1	12	38.23	9	38.31	16.5	9.3
2	9	33.12	5	34.66	10.3	7.8
3	10	32.71	8	36.88	12.2	8.2

Table 2. Raman frequencies and assignments for PPRu hybrids.

Raman shift (cm^{-1})	Assignments	Raman shift (cm^{-1})	Assignments
330	Por plane	1405	Imidazole ring
411	Por plane + Ag–N	1451	Phen
814	N^+–CH_3	1491	Imidazole ring
990	Pyridine ring	1568	Imidazole ring
1091	Pyrrole ring	1604	Phen
1196	Pyridine ring + N^+–CH_3	2540	Pyridine ring
1214	Pyrrole ring	2572	CH_2
1264	Imidazole ring	2700	CH_2
1308	Phen	2939	CH_2

The melting curves of CT DNA in the absence and presence of compounds are presented in figure 5. Under the present experimental conditions, the melting curve has a transition and the T_m value of free double-stranded CT DNA is (60.6 ± 0.2) °C. When mixed with the compounds, the observed melting temperatures of CT DNA increase to different extents and the increases of T_m (ΔT_m) are summarized in table 1.

From table 1, we find that the values of ΔT_m in the presence of **1**, **2** and **3** are relatively large (16.5 °C, 10.3 °C and 12.2 °C, respectively), suggesting that the compounds may interact with DNA in an intercalative mode and have strong DNA binding affinities. This result is expected since the absorption and ICD spectra have indicated that the porphyrin moieties of these hybrids intercalated into DNA.

It is worth noting that the increase about all these hybrids are even larger than that of 5-(4-hydroxyphenyl)-10,15,20-tris(4-N-methylpyridiniumyl)porphyrin triiodide (namely [HTMPyP]I_3), which is the porphyrin body of these compounds and has been proved to intercalate into DNA through its porphyrin plane [10]. It is reasonable if one considers from this result that besides the perfect DNA intercalation of Por moieties, the polypyridyl moieties in the PPRu hybrids also intercalate into DNA duplex. However, it is unexpected that **2** with largest polypyridyl plane did not show the biggest ΔT_m value. We suppose that the polypyridyl moiety in **2** only partially intercalates into DNA bases because of its too large planar area and the steric hindrance between porphyrin and ploypyridyl moieties which result from the large pip bulk. The results of thermal denaturation further argue for the fully bis-intercalative DNA binding mode of **1** and **3**, while the polypyridyl moiety in **2** may partially intercalate.

3.2.6. SERS investigation. To further probe the DNA binding modes of these hybrids, the SERS method was employed. SERS is a powerful tool to clarify the exact DNA binding mode of hybrids with multi binding sites since different moieties in the molecules could exhibit distinct SERS signals [10, 11]. The metal colloids can be adapted for the application in the study of biological objects, because they do not modify to a great extent the structures of biological molecules adsorbed on their surface [38].

The SERS spectra of the hybrids in the absence and presence of CT DNA are shown in figure 6. Table 2 summarizes the main SERS bands of the compounds and their assignments. Figure 6 also exhibits the SERS spectrum of free CT DNA. It is found that no substantial SERS signal is given by free CT DNA, since the Ag colloids have negative charges on their surface, which repulses the adsorption of negative-charged DNA molecules [39].

Curves 1–3 in figure 6 show the SERS spectra of the compounds in the absence of DNA, which are very similar to each other. This similarity in the SERS spectra results from the quite similar molecular structure of these compounds. Curves 1′-3′ in figure 6 show the SERS spectra of complexes of PPRu hybrids at 5 μM with CT DNA at 150 μM. SERS spectra of these compounds in the presence of DNA are very different from those in the absence of DNA. For all the compounds, most bands of the compound/DNA complexes significantly decreased, indicating that the interactions of PPRu compounds with DNA can largely reduce the amount of compounds adsorbed on Ag colloids [39]. Especially, the band at 330 cm^{-1} is mainly assigned to the bending vibration of the Por ring and is the marker band of the free-base Por compounds in the SERS-active system; the disappearance of this band is due to the decrease of free-base Por molecules surrounding Ag colloids after the interaction between PPRu compounds and DNA [39–42]. The disappearance of bands centered at 411, 814 and 1091 nm, which are attributed to the porphyrin, also indicates that

the porphyrin moieties of the compounds are protected by DNA from adsorbing on Ag particles [39–42]. These results illustrated that the porphyrin moieties of these compounds employed intercalation or groove binding DNA binding modes which could make the porphyrin moiety be well embedded in the DNA structures.

Meanwhile, upon binding with DNA, the strong signals centered at 1308, 1451 and 1604 cm^{-1}, which were the characteristic bands of phen structures (in both Ip and phen ligand), completely vanished for **1** [44, 45], indicating that the polypyridyl Ru(II) moiety of **1** well intercalated in DNA molecules, since it was reported that the disappearance of the Raman peak associated with any part of the molecule can be explained by a strong π–π stacking interaction between the part and DNA [46]. However, in the case of **2**, these peaks attributed to phen structures, as well as those peaks attributed to the imidazole plane (1405, 1491 and 1568 nm), could still be observed although the intensities were greatly decreased and exhibited a broad featureless nature. This result indicated that the pip ligand of **2** may only partially embed into DNA structures and thus was not well protected by DNA duplexes. As for **3**, the peaks attributed to pyridine ring vanished, indicating that the bpy ligand intercalates into DNA bases. Meanwhile, the remaining bands centered at 2940 nm, which can be ascribed to the carbon links in the molecule, suggests that the flexible carbon links may be still exposed in the solvent.

Moreover, the chosen protocol for the SERS sample preparation allows the DNA-compound adduct to be formed before its addition to the colloid solution (see Experimental). Consequently, the spectral changes confirm that the cationic PPRu hybrid efficiently binds to DNA even in Ag sols. In this medium, the preference of cationic compound for polyanionic DNA prevails over negatively charged Ag nanoparticles. This also reveals the tight binding affinities between the cationic drugs and DNA [39].

3.2.7. Equilibrium dialysis. In the absence of X-ray structural data, the hydrodynamic method is frequently employed since it is sensitive to changes in the length of DNA in solution [4]. However, attempts to see the DNA change at higher viscosity for the cationic PPRu hybrids were not successful because red precipitates were observed visually under the drug concentrations needed in this experiment. This phenomenon is common in the viscosity research of cationic macrocycle drugs with DNA and can be ascribed to the external binding mode between the positive macrocycles and the negative phosphate backbone [10, 46]. Equilibrium dialysis experiments were thus carried out to investigate the DNA binding behaviors of these compounds at a [PPRu]/[DNA] ratio of 0.1 and the results are summarized in figure 7 as a histogram. As shown in figure 7, under identical experimental conditions, the amounts of the hybrids bound to CT DNA decreased in the order of **1** > **3** > **2**, in agreement with the results from absorption titration and thermal denaturation studies above, and should be closely correlated with their DNA binding affinities [47].

3.2.8. Competitive binding experiments. The above experimental results suggest that there are some interactions between these compounds and DNA. In order to compare quantitatively, their binding affinity constants (K_b) to CT DNA have to be measured. UV–Vis titration is not suitable to determine K_b of compounds with multiple binding sites [10, 11, 48, 49] and thus the fluorescence spectrum was used to measure K_b by competition between EB and the studied compounds for binding to DNA. This method measures the decrease of fluorescence of EB bound to DNA in the presence of the compound of interest.

It can be used for all compounds having a good affinity for DNA whatever their binding modes may be, because it only measures the ability of a compound to prevent intercalation of EB into DNA [10, 11, 48].

The EB competitive binding experiments were carried out and quenching plots are given in figure 8. The quenching plots of I_0/I *vs* [PPRu]/[DNA] are in agreement with the linear Stern–Volmer equation with slopes of 5.90, 4.88, 5.12 for **1**, **2** and **3**, respectively. We also learn from figure 8 that 50% of EB molecules were replaced from DNA-bound EB at a concentration ratio of [PPRu]/[EB] = 1.06, 1.28 and 1.22 for **1**, **2** and **3**, respectively. By taking K_b of 1.0×10^7 M^{-1} for EB under this experimental condition [50], the K_b of **1**, **2** and **3** were derived at 9.3×10^6 M^{-1}, 7.8×10^6 M^{-1} and 8.2×10^6 M^{-1} (K_b(EB)/1.06, K_b(EB)/1.28 and K_b(EB)/1.22), respectively [10, 46], following an order of **1** > **3** > **2**. The planar area of the Ru(II) ligand played an important role in determining the K_b values. Small ligand planar area was proved unfavorable to the tight interaction with DNA (hybrid **3**), while a too large area may encounter steric hindrance between the two moieties in the hybrids and thus could not completely intercalate into DNA bases. Proper ligand area seems very significant in obtaining a high K_b value and ideal DNA binding mode.

3.3. *DNA photocleavage*

3.3.1. DNA photocleavage under different wavelength range. We comparably investigated the photocleavage of pBR322 plasmid DNA by the studied compounds under irradiation with visible light (at porphyrin's excited wavelength) or ultraviolet light (at polypyridyl Ru(II)'s excited wavelength) and the results are presented in figure 9. Without irradiation, no substantial cleavage of DNA was observed for all the compounds. However, these cationic PPRu hybrids could effectively photocleave DNA under irradiation with both visible and ultraviolet light, and the DNA-photocleavage activities of **1** and **3** are higher than that of **2**. It seems that bis-intercalative binding mode and large K_b are advantageous to effective DNA-photocleavage. These results are consistent with previous reports on the relationship between DNA binding and photocleavage of small molecules [9–11, 34]. On the other hand, all the Ru(II) complexes which are reported as DNA photocleaving drugs in recent years could only cleave DNA under ultraviolet light [17–24]. However, the new PPRu hybrids with double cleavage sites have a broader wavelength range (both visible and ultraviolet light). Thus, they are considered as more useful photonucleases than the traditional Ru(II) complexes with a single DNA photocleaving site.

3.3.2. Mechanism of DNA photocleavage. Here we investigate the influence of different potentially inhibiting agents on the DNA photocleavage of the PPRu hybrids. Figure 10 shows the DNA photocleavage by **1** in the presence of inhibiting agents. The percentage of Form II DNA after photoirradiation in the presence of **1** decreased by addition of NaN_3, which is known to be a scavenger of $^1O_2$. When the sample solutions were thoroughly degassed with nitrogen gas and maintained under N_2 during the experiment, the DNA photocleavage was greatly inhibited as compared with that in air. In addition, the photocleavage ability was substantially enhanced by replacing the reaction media H_2O by 70% D_2O, which makes the life span of $^1O_2$ longer. These results suggest that the pathway to produce Form II DNA is aerobic and $^1O_2$ are the reactive species responsible for the DNA photocleavage. On the other hand, the hydroxyl radical is hardly involved in the DNA

Table 3. The slopes (S) of the plots of bleached absorption of DPBF by photosensitization of PPRu.

PPRu	**1**	**2**	**3**
S	0.33	0.22	0.31

photocleavage by **1** since the addition of ethanol, methanol and DMSO, which are known as scavengers of hydroxyl radical, did not significantly affect the percentage of Form II DNA. Similar cases were observed for **2** and **3**.

Because $^1O_2$ was clearly responsible for the DNA photocleavage by the hybrids in our system, photosensitized productivity of $^1O_2$ was estimated quantitatively by measuring the decomposition of 1,3-diphenylisobenzofuran (DPBF). DPBF directly reacts with $^1O_2$ and subsequently decomposes to 1,2-dibenzoylbenzene. Absorbance of DPBF (30 mM) at 415 nm linearly decreased in the presence of each porphyrin as illumination time increased. The slopes of the plots of bleached absorption of DPBF versus illumination time are listed in table 3. The value of the slope for **2** is smaller than those of **1** and **3**, indicating that the larger planar area is disadvantageous in $^1O_2$ production. Since it has been reported that the self-aggregation of molecules may decrease the $^1O_2$ productivity and better planarity always favors self-aggregation [51, 52], it is understandable that **2** with largest planar area produce $^1O_2$ less efficiently and thus has lower DNA photocleavage efficiency than **1** and **3**.

4. Conclusion

This paper introduced a series of cationic PPRu hybrids with different polypyridyl planes and their binding behaviors with CT DNA as well as their photocleavage activities to plasmid DNA. Through spectral and thermodynamic methods, it is found that the polypyridyl units in **1** and **3** intercalate into DNA bases, whereas the largest polypyridyl plane in **2** only partially intercalates because of steric interactions. Proper planar area seems very significant in designing such drugs with multiple interactive sides. However, in the absence of X-ray structural data, the exact DNA binding mode of these compounds could not be concluded only on the basis of the spectral results. Compared with Ru(II) complexes which were frequently reported in recent years [17–24], these new cationic PPRu hybrids exhibit richer binding and photocleaving DNA, such as more DNA binding sites and broader DNA photocleaving wavelength range. These results may facilitate the design of highly-efficient antitumor antibiotics.

Funding

This work was financially supported by the National Nature Science Foundation of China [grant number 21101033] and Guangdong Pharmaceutical University.

References

[1] L. Wolf. *Chem. Eng. News*, **89**, 10 (2011).
[2] F. Schmitt, P. Govindaswamy, G. Fink, W.H. Ang, P.J. Dyson, L.J. Jeanneret, B. Therrien. *J. Med. Chem.*, **51**, 1811 (2008).

[3] X. Chen, L. Hui, D.A. Foster, C.M. Drain. *Biochemistry*, **43**, 10918 (2004).
[4] T. Ohyama, H. Mita, Y. Yamamoto. *Biophys. Chem.*, **113**, 53 (2005).
[5] J.O. Kim, Y.A. Lee, B. Jin, T. Park, R. Song, S.K. Kim. *Biophys. Chem.*, **111**, 63 (2004).
[6] Y. Deng, C.K. Chang, D.G. Nocera. *Angew. Chem., Int. Ed.*, **39**, 1066 (2000).
[7] D.R. McMillin, A.H. Shelton, S.A. Bejune, P.E. Fanwick, R.K. Wall. *Coord. Chem. Rev.*, **249**, 1451 (2005).
[8] S. Wu, Z. Li, L.G. Ren, B. Chen, F. Liang, X. Zhou, T. Jia, X.P. Cao. *Bioorg. Med. Chem.*, **14**, 2956 (2006).
[9] P. Zhao, L.C. Xu, J.W. Huang, K.C. Zheng, J. Liu, H.C. Yu, L.N. Ji. *Biophys. Chem.*, **134**, 72 (2008).
[10] P. Zhao, L.C. Xu, J.W. Huang, B. Fu, H.C. Yu, W.H. Zhang, J. Chen, J.H. Yao, L.N. Ji. *Bioorg. Chem.*, **36**, 278 (2008).
[11] P. Zhao, L.C. Xu, J.W. Huang, B. Fu, H.C. Yu, L.N. Ji. *Dyes Pigm.*, **83**, 81 (2009).
[12] I. Bratsos, S. Jedner, T. Gianferrara, E. Alessio. *Chimia*, **61**, 692 (2007).
[13] X. Meng, M.L. Leyva, M. Jenny, I. Gross, S. Benosman, B. Fricker, S. Harlepp, P. Hébraud, A. Boos, P. Wlosik, P. Bischoff, C. Sirlin, M. Pfeffer, J.-P. Loeffler, C. Gaiddon. *Cancer Res.*, **69**, 5458 (2009).
[14] T.F. Chen, Y.N. Liu, W.J. Zhen, J. Liu, Y.S. Wong. *Inorg. Chem.*, **49**, 6366 (2010).
[15] Y.J. Liu, C.H. Zeng, H.L. Huang, L.X. He, FHWu Eur. *J. Med. Chem.*, **45**, 564 (2010).
[16] J.G. Liu, Q.L. Zhang, X.F. Shi, L.N. Ji. *Inorg. Chem.*, **40**, 5045 (2001).
[17] Y.J. Liu, C.H. Zeng, F.H. Wu, J.H. Yao, L.X. He, H.L. Huang. *J. Mol. Struct.*, **932**, 105 (2009).
[18] P.U. Maheswari, V. Rajendiran, M. Palaniandavar, R. Parthasarathi, V. Subramanian. *J. Inorg. Biochem.*, **100**, 3 (2006).
[19] T. Biver, C. Cavazza, F. Secco, M. Venturini. *J. Inorg. Biochem.*, **101**, 461 (2007).
[20] L. Xu, N.J. Zhong, Y.Y. Xie, H.L. Huang, Z.H. Liang, Z.Z. Li, Y.J. Liu. *J. Coord. Chem.*, **65**, 55 (2012).
[21] X.W. Liu, Y.D. Chen, L. Li. *J. Coord. Chem.*, **65**, 3050 (2012).
[22] Y.Y. Xie, G.B. Jiang, J.H. Yao, G.J. Lin, H.L. Huang, X.Z. Wang, Y.J. Liu. *J. Coord. Chem.*, **66**, 2423 (2013).
[23] H. Paul, T. Mukherjee, M. Mukherjee, T.K. Mondal, A. Moirangthem, A. Basu, E. Zangrando, P. Chattopadhyay. *J. Coord. Chem.*, **66**, 2747 (2013).
[24] M. Shilpa, C.S. Devi, P. Nagababu, J. Naveena, L. Latha, R. Pallela, V. Rao. Janapala, K. Aravind, S. Satyanarayana, *J. Coord. Chem.*, **66**, 1661 (2013).
[25] K. Davia, D. King, Y. Hong, S. Swavey. *Inorg. Chem. Commun.*, **11**, 584 (2008).
[26] Z.M. Xu, S. Swavey. *Inorg. Chem. Commun.*, **14**, 882 (2011).
[27] Y.N. Liu, T.F. Chen, Y.S. Wong, W.J. Mei, X.M. Huang, F. Yang, J. Liu, W.J. Zheng. *Chem. Biol. Interact.*, **183**, 349 (2010).
[28] M.E. Reichmann, S.A. Rice, C.A. Thomas, P. Doty. *J. Am. Chem. Soc.*, **76**, 3047 (1954).
[29] J. Chen, J.M. Hu, Z.S. Xu, R.S. Sheng. *Appl. Spectrosc.*, **47**, 292 (1993).
[30] C.J. Sansonetti, M.L. Salit, J. Reader. *Appl. Opt.*, **35**, 74 (1996).
[31] P. Zhao, L.C. Xu, J.W. Huang, K.C. Zheng, B. Fu, H.C. Yu, L.N. Ji. *Biophys. Chem.*, **135**, 102 (2008).
[32] J.W. Huang, J.F. Liu, X.D. Jiao, L.N. Ji. *Chem. J. Chin. Univ.*, **16**, 163 (1995).
[33] J.Z. Wu, B.H. Ye, L. Wang, L.N. Ji, J.Y. Zhou, R.H. Li, Z.Y. Zhou. *J. Chem. Soc., Dalton Trans*., 1395 (1997).
[34] R.F. Pasternack, E.J. Gibbs, J.J. Villafranca. *Biochemistry*, **22**, 2406 (1983).
[35] J.S. Trommel, L.G. Marzilli. *Inorg. Chem.*, **40**, 4374 (2001).
[36] L.N. Ji, X.H. Zou, J.G. Liu. *Coord. Chem. Rev.*, **216–217**, 513 (2001).
[37] C.V. Kumar, J.K. Barton, N.J. Turro. *J. Am. Chem. Soc.*, **107**, 5518 (1985).
[38] J. De Groot, R.E. Hester. *J. Phys. Chem.*, **91**, 1693 (1987).
[39] C.Y. Wei, G.Q. Jia, J.L. Yuan, Z.C. Feng, C. Li. *Biochemistry*, **45**, 6681 (2006).
[40] M. Procházka, P.Y. Turpin, J. Sÿtěpánek, J. Bok. *J. Mol. Struct.*, **221**, 482 (1999).
[41] S.N. Terekhov, S.G. Kruglik, V.L. Malinovskii, V.A. Galievsky, V.S. Chirvony, P.Y. Turpin. *J. Raman Spectrosc.*, **34**, 868 (2003).
[42] Y.C. Ning. *Structure Identification of Organic Compounds and Organic Spectroscopy*, pp. 485–498., Science Press, Tsinghua (1991).
[43] E. Gaudry, J. Aubard, H. Amouri. G. Lévi1, C. Cordier, *Biopolymers*, **82**, 399 (2006).
[44] J.R. Schoonover, W.D. Bates, T.J. Meyer. *Inorg. Chem.*, **34**, 6421 (1995).
[45] W. Chen, C. Turro, L.A. Friedman, J.K. Barton, N.J. Turro. *J. Phys. Chem. B*, **101**, 6995 (1997).
[46] M.E. Anderson, A.G.M. Barrett, B.M. Hoffman. *J. Inorg. Biochem.*, **80**, 257 (2000).
[47] Y. Ishikawa, A. Yamashita, T. Uno. *Chem. Pharm. Bull.*, **49**, 287 (2001).
[48] M.A. Sari, J.P. Battioni, D. Dupre, D. Mansuy, J.B. Lepecq. *Biochemistry*, **29**, 4205 (1990).
[49] T. Jia, Z.X. Jiang, K. Wang, Z.Y. Li. *Biophys. Chem.*, **119**, 295 (2006).
[50] Y.Y. Fang, B.D. Ray, C.A. Caussen, K.B. Lipkowitz, E.C. Long. *J. Am. Chem. Soc.*, **126**, 5403 (2004).
[51] Y. Ishikawa, N. Yamakawa, T. Uno. *Bioorg. Med. Chem.*, **10**, 1953 (2002).
[52] N. Yamakawa, Y. Ishikawa, T. Uno. *Chem. Pharm. Bull.*, **49**, 1531 (2001).